A COAXIAL TE_{011} CAVITY AND A SYSTEM TO MEASURE DC AND RF PROPERTIES OF SUPERCONDUCTORS*

G. Ciovati#, P. Kneisel, G. R. Myneni, M. Morrone, R. Bundy, B. Clemens, T. Elliott, G. Slack, L. Turlington, Jefferson Lab, Newport News, VA 23606, USA
J. Mondal, Accelerator & Pulse Power Division, BARC, Mumbai, 400 085, India

Abstract

A coaxial niobium cavity has been designed and built where the center conductor consists of a removable sample. In addition, a system to measure properties such as magnetization, penetration depth, critical temperature and thermal conductivity on the same cylindrical sample has been designed and built. The purpose of this effort is to investigate possible correlations between DC and RF properties of superconductors. In this contribution, the design of the various components is discussed and the test results on a niobium sample obtained so far are presented.

INTRODUCTION

For many years attempts have been made to correlate the performance of niobium radio-frequency (RF) cavities with material properties [1] and in particular properties of the metal-oxide interface. In most cases, the surfaces have been investigated on samples, which had no resemblance to the cavities, but were supposedly treated in the same way as the cavities. Another discrepancy between these two different investigations is the size of the surface area: samples are typically ~ cm^2, whereas cavity surfaces can be many hundreds of square cm.

In 1973 a paper was published at BNL [2], which proposed to use a coaxial TE_{011} cavity as a vehicle to measure metallurgical properties and superconducting RF breakdown fields on the same sample. Besides the obvious investigation of different surface treatments for niobium samples, this cavity could also be used for other materials of interest. In addition we built a simple system to measure the magnetization curve, the penetration depth, pinning properties and thermal conductivity on the same sample, which may allow finding correlations between DC and RF superconducting properties. The sample is also small enough to fit into any surface analytical instrument for further investigation.

COAXIAL TE_{011} CAVITY

Cavity Design and Fabrication

The TE_{011} cavity has a simple "pill-box" geometry, shown in Fig. 1a, and a coaxial cylindrical sample, 6 mm in diameter and 120 mm long (Fig. 1), is inserted in the middle of the top plate. The sample is hollow to allow cooling by the superfluid He. This geometry allows an analytical calculation of fields and frequencies of the various modes. The main electromagnetic parameters of the TE_{011} mode are listed in Table 1. The maximum surface magnetic field occurs in the middle of the sample, while it is in the middle of the cylindrical portion of the cavity without sample. The ratio of the magnetic field at these two locations is 2.38. For the input and output coupling, 10 mm diameter holes were cut from the top plate and they are off-center from the coupling tube, which allows coupling to the TE_{011} mode using coaxial antennae.

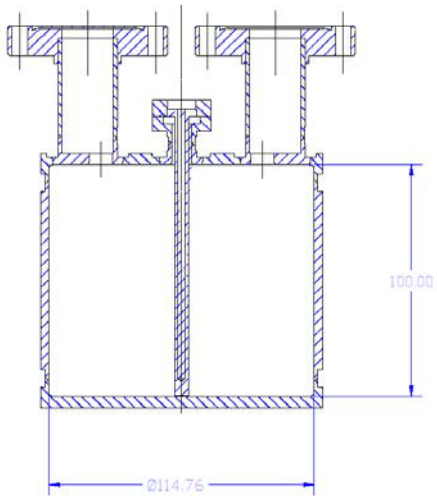

Figure 1: Geometry of the coaxial TE_{011} cavity. Dimensions are in mm.

Table 1: Main electromagnetic parameters of the TE_{011} mode for the coaxial cavity shown in Fig. 1. P_{sample}/P_{total} is the ratio of the power dissipated on the sample over the total dissipated power per unit R_s.

Frequency (GHz)	3.544
$B_p/\sqrt{U}$ (mT/√J)	151.8
$G = Q_0 R_s$ (Ω)	623.8
P_{sample}/P_{total}	19.3%

The cavity was fabricated from RRR > 200 Nb. The cylindrical part (fine grain Nb from Wah Chang) was fabricated by rolling and electron-beam welding (EBW), the top and bottom plates were machined from Nb disks (the bottom plate is from CBMM large grain Nb) and the various parts were joined by EBW. About 50 μm were

#gciovati@jlab.org

etched from the Nb parts by buffered chemical polishing (BCP) with HF, HNO_3 and H_3PO_4 in 1:1:1 ratio prior to the final weld of the bottom round plate. The flanges for the input and output probes were 2 ¾" Conflat made of Nb55Ti joined to the coupling tubes by EBW. The sample was machined from a Nb rod, a 2 mm diameter hole was drilled in the center from both sides, then the tip and the base were joined to the cylinder by EBW. Figure 2 shows a picture of the cavity and sample as fabricated. We chose an "all-welded" design to avoid potential losses at a flanged endplate.

Figure 2: Picture of the cavity (left) and sample (right) as fabricated.

RF Test Results

One difficulty with the surface preparation of this cavity is represented by the limited access to the internal surface, as there are only two small coupling holes and an even smaller hole in the center. The typical preparation consists of:

- ultrasonic degreasing in a soapy solution for 20 min.
- BCP in 1:1:4 ratio, removing about 15 µm of material, after initial removal of 40 µm following the cavity fabrication. We chose to use 1:1:4 rather than the more common 1:1:1 or 1:1:2 to slow down further the reaction rate, since the acid is enclosed in the cavity volume and it is not agitated. The material removal rate of a fresh 1:1:4 solution was measured to be about 1.3 µm/min by weight loss on a Nb sample.
- Rinse ten times with ultrapure water.
- Drying in class 100 clean room with a filtered N_2 gun. Assembly of the input and output probe. A "T" section in the input coupler line provided the additional port for the cavity evacuation. The Nb sample was sealed to the cavity with indium wire.
- Evacuation to ~ 10^{-7} mbar on the vertical test stand.

The cavity was initially tested without sample, to obtain a baseline performance of the cavity itself, and the center opening was closed with a Nb disk. At 2 K, the TM_{111} mode, which is theoretically degenerate with the TE_{011} mode, was at a 6.4 MHz higher frequency and had stronger coupling than the TE mode. The high-power RF test was limited by multipacting (MP) at $B_p \cong 18$ mT. The distance between the tip of the input antenna and the top plate was about 2 mm and that was suspected to be the region where MP occurred. The antenna was shortened by 4.25 mm and 15 µm were removed from the inner cavity surface by BCP. The low field Q_0 at 2 K was only 1.5×10^7 and we suspected Q-disease due to hydrogen contamination during the chemical etching. The cavity was degassed in a vacuum furnace at 600 °C for 10 h, followed by 20 µm etching. After rinsing with ultrapure water, the cavity was rinsed with methanol. The RF test results (Test 3 in Fig. 3) still showed MP at $B_p \cong 12$ mT which processed after about 1 h of applying RF. The quality factor dropped rapidly at higher field up to 18 mT where it quenched.

The diameter of the input antenna was reduced by 1.25 mm and 20 µm were etched from the inner cavity surface. The RF test at 2 K (Test 4 in Fig. 3) still showed a degradation of Q_0 with increasing RF field and MP at $B_p \cong 18$ mT. The "T" section with the pump-out port was moved to the output probe side and 5 µm were etched from the cavity. MP started at $B_p \cong 20$ mT (Test 5 in Fig. 3). A magnetic loop was made to replace the input antenna and in the following RF test (Test 6 in Fig. 3) MP occurred at about $B_p \cong 22$ mT.

We finally decided to test the cavity with a Nb sample which was etched by about 100 µm with BCP 1:1:1. Three MP barriers were encountered: at $B_p \cong 34$ mT, which processed rather quickly, at $B_p \cong 42$ mT which processed after longer time (~ 20 min) and a hard one at $B_p \cong 50$ mT (Test 7 in Fig. 3). This value of peak field on the sample corresponds to 21 mT peak field on the cavity, which is consistent with the field level at which MP was occurring in the cavity without sample.

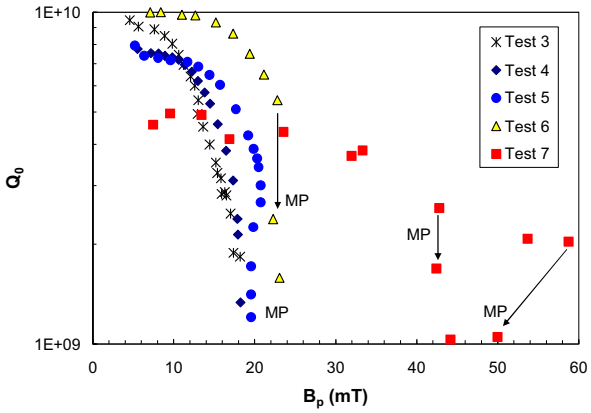

Figure 3: Summary of RF tests at 2 K on the TE_{011} cavity. Refer to the text for details about the various tests. Only Test 7 was done with the coaxial Nb sample.

SYSTEM FOR MEASUREMENTS OF MATERIAL SUPERCONDUCTING PROPERTIES

System Design

A system to measure the magnetization curve, the thermal conductivity, the penetration depth and the surface pinning characteristics of the sample rod was designed and built. A heater made with constantan wire glued on a Cu block with Epoxy is clamped near the base of the sample. Two calibrated Cernox resistors are soldered with indium on two small Cu blocks which are clamped to the rod at a distance of about 40 mm. A pick-up coil (~ 200 turns, 0.29 mm diameter Cu wire) is inserted in the middle of the sample, between the two Cernox. The sample is clamped on a Cu block which is inserted in a copper tube and sealed with indium wire. A stainless steel 2 ¾" Conflat flange was brazed on the other end of the tube. The tube is bolted to a "T" section where a flange with feedthrough connectors is bolted on the side. The assembly is bolted to the vacuum line on a vertical test stand (the pressure in the Cu tube is ~ 10^{-5} mbar at 4.3 K). Some heat shields were inserted in the vacuum line to minimize radiation losses. A superconducting magnet up to 1 T (0.1% field homogeneity over the sample length) made by Cryomagnetics surrounds the Cu tube carrying the sample. Figure 4 shows a schematic of the system, while a picture of it is shown in Fig. 5.

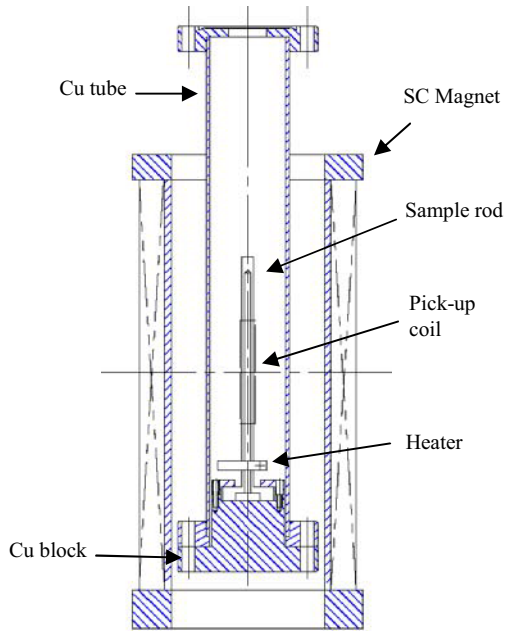

Figure 4: Schematic of the system for measurements of superconducting properties of the sample.

Measurement Methods and Results

The thermal conductivity as a function of the average temperature of the sample is calculated using Fourier's law where the power supplied to the heater, P, the temperature difference, ΔT, the distance d between the two Cernox, and the cross-sectional area of the sample A are measured:

$$\kappa = \frac{P}{\Delta T}\frac{d}{A} \qquad (1)$$

The heater power and the sample temperature are controlled with a LakeShore 332 Temperature Controller. Figure 6 shows a plot of $\kappa(T)$ for a polycrystalline Nb rod after heat-treatment in a vacuum furnace at 600 °C for 10 h and a total of 140 µm material removal by BCP 1:1:1.

Figure 5: Picture of the assembly for sample measurements.

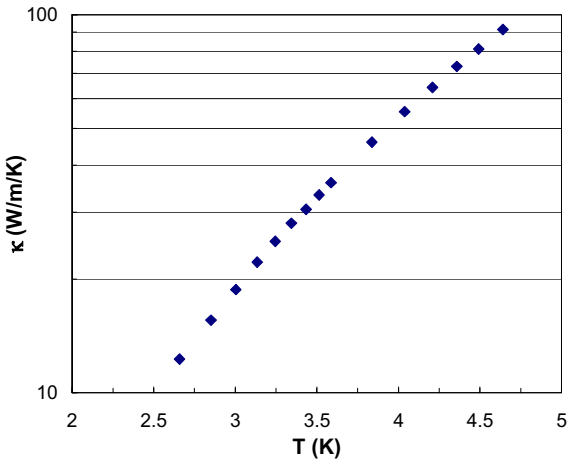

Figure 6: Thermal conductivity as a function of temperature measured on a polycrystalline Nb rod after heat-treatment at 600 °C/10 h and a total of 140 µm material removal by BCP 1:1:1.

The magnetization of the sample as a function of the applied field is obtained by linearly ramping the current in the superconducting magnet (the field-to-current ratio is 12.9 mT/A) at a rate of about 0.1 A/s while measuring the voltage from the pick-up coil with a Keithley 2182 nanovoltmeter. The magnetization is calculated from the following formula [3]:

$$M(B_a) = \frac{-1}{1-N_D}\int_0^{B_a} \frac{V(B_a') - V_n}{V_s - V_n} dB_a' \qquad (2)$$

where V_n and V_s are the voltages in the normal and

superconducting state respectively and N_D is the demagnetization factor, estimated to be about 0.007 for our samples.

A Power Ten power supply (0-10 V, 0-100 A) controlled by an American Magnetics 412 Programmer, remotely controlled by a PC, provides the current to the superconducting solenoid. Figure 7 shows the magnetization curve measured at 4.2 K on a polycrystalline Nb rod after heat-treatment in a vacuum furnace at 600 °C for 10 h and a total of 140 µm material removal by BCP 1:1:1. The values of the lower and upper critical field at 4.3 K are about 130 mT and 260 mT, respectively.

For calibration purposes, we also measured the critical field B_c as a function of temperature for an Indium rod (99.99% purity) made by melting the Indium in a stainless steel mold. The data, showed in Fig. 8, were fitted with the classical formula

$$B_c(T) = B_c(0)\left(1-\frac{T^2}{T_c^2}\right) \qquad (3)$$

and resulted in T_c = 3.35 ± 0.03 K and $B_c(0)$ = 27 ± 2 mT, in good agreement with published data [4].

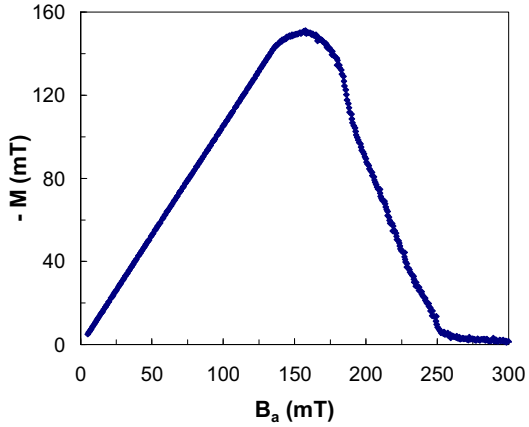

Figure 7: Magnetization curve measured on a Nb rod at 4.3 K after heat-treatment at 600 °C/10 h and a total of 140 µm material removal by BCP 1:1:1.

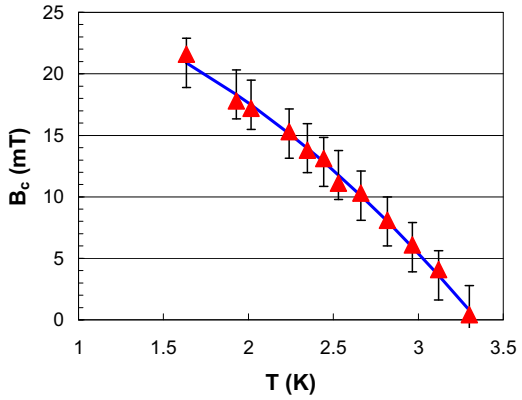

Figure 8: Critical magnetic field as a function of temperature measured on a Indium rod, 99.99% purity. The solid line is a least-square fit with Eq. (3).

By connecting the pick-up coil as part of a L-C oscillator, it is possible to measure the changes of the penetration depth as a function of the applied DC magnetic field by measuring the changes of the oscillator's resonant frequency f_0 (the base frequency is 270 kHz, sampling up to a depth ~10 µm) while slowly ramping up and down the magnetic field [5]. This method, which was applied in Ref. [5] for Nb studies, provides information about surface pinning and allows measuring the surface critical field B_{c3}. Figure 9 shows a measurement of the frequency change $\Delta f(B_a)$ at 4.3 K for the Nb rod used in Fig. 7. The irreversibility of the curve between B_{c1} and B_{c2} is an indication of significant surface pinning. B_{c3} is about 510 mT.

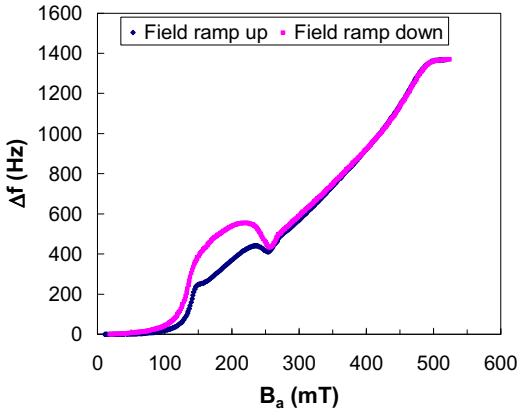

Figure 9: Change of resonant frequency, which is proportional to the 270 kHz small-field penetration depth at 4.3 K, as a function of the applied DC magnetic field parallel to the surface of a Nb rod.

It is also possible to measure the change of penetration depth $\Delta\lambda$ as a function of temperature by slowly warming up the cryostat to 10 K while measuring the change of resonant frequency of the L-C oscillator, due to changes of the inductance of the coil surrounding the sample (Schawlow and Devlin method [6]). This method also allows measuring the critical temperature T_c. $\Delta\lambda$ is calculated from Δf using the following formula:

$$\Delta\lambda(T) = -\frac{1}{Gr}\frac{\Delta f(T)}{f_0^3} \qquad (4)$$

where r is the diameter of the rod, f_0 is the resonant frequency at 4.3 K and G is a geometrical constant obtained from a linear fit of $1/f_0^2$ vs. r^2. By fitting $\Delta\lambda(T)$ with a BCS theory code [7] it is possible to estimate the value of the penetration depth at 0 K, λ_0. Figure 10 shows a plot of $\Delta f(T)$ for the Nb rod of Fig. 7 while Fig. 11 shows the $\Delta\lambda(T)$ fitted with the BCS theory code. λ_0 = 52 ± 11 nm and T_c = 9.31 ± 0.01 K resulted from the fit.

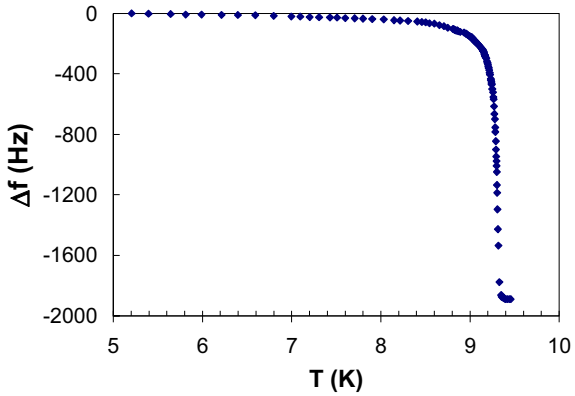

Figure 10: Frequency change as a function of temperature measured on the Nb rod of Fig. 7.

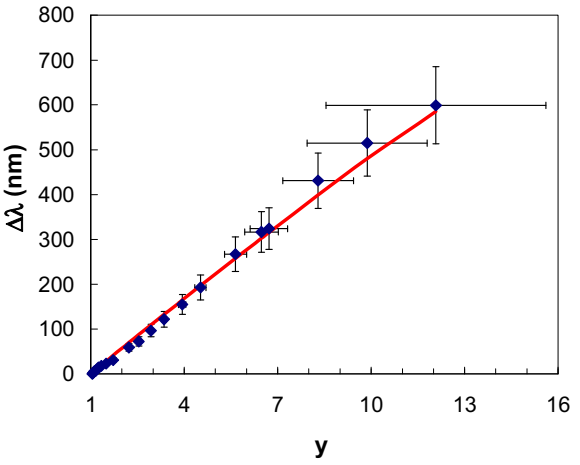

Figure 11: Δλ as a function of $y = 1/\sqrt{1-(T/T_c)^4}$ calculated with Eq. (4). The solid line is a least-square fit with the BCS theory code.

CONCLUSIONS AND FUTURE PLANS

A coaxial cavity to measure RF breakdown fields and an integrated system to measure superconducting properties, such as the critical temperature, DC critical fields penetration depth, and thermal properties such a thermal conductivity were designed and built. The MP problems in the coaxial cavity were quite unexpected, since the TE_{011} mode has no electric field component normal to the surface. The MP barrier at $B_p \cong 18$ mT in the cavity without sample was very strong and could not be processed with RF processing. The region where MP occurs is unclear. The coupling tube and antennae were suspected, although the MP occurs at very low input power levels (1-2 W) and did not change significantly when moving from an electric-type coupling (coaxial antenna) to a magnetic-type (loop). 3D simulations with Microwave Studio did not show significant field enhancement at the coupling holes on the top plate of the cavity. 3D multipacting calculations with VORPAL are currently under way at Tech X [8], to help identifying the possible MP locations. We think that the inability to have easy access to the inner surface of the cavity, which reduces the ability to do a proper chemical etching and cleaning, may contribute to this problem. Therefore we plan to cut the bottom plate of the cavity and make it so that it can be flanged to the rest of the cavity. Indium wire will be used for sealing of the cavity.

The integrated system for sample measurements is well functioning, as shown by the preliminary data reported in this contribution, and we plan to begin a systematic investigation of high-purity Nb samples subjected to different treatments, such as post-purification, hydrogen degassing and low temperature baking.

REFERENCES

[1] P. Kneisel, "Surface Characterization of Bulk Nb: What Has Been Done, What Has Been Learnt?", Proc of the 11th SRF Workshop, Travemünde, September 2003, paper TuO02.

[2] W. Bauer, S. Giordano and T. Luhman, Brookhaven National Laboratory Report 18186, AADD 73-11, 1973.

[3] N. J. Imfeld, W. Bestgen and L. Rinderer, J. Low Temp. Phys. 60 (1985) 223.

[4] D. K. Finnemore and D. E. Mapother, Phys. Rev. 140 No. 2A (1965) 507.

[5] P. Kneisel, O. Stolz and J. Halbritter, J. Appl. Phys. 45 No. 5 (1974) 2296.

[6] A. L. Schawlow and G. E. Devlin, Phys. Rev. 113 No. 1 (1959) 120.

[7] J. Halbritter, Internal Report FZK 3/70-6 (1970).

[8] C. Nieter et al., "Self-Consistent Simulations of Multipacting in Superconducting Radio Frequencies", PAC'07, Albuquerque, June 2007, p. 769.